Differing impacts of resolution changes in latitude and longitude on the mid-latitudes in the LMDZ Atmospheric GCM

Virginie Guemas[1] and Francis Codron [2]

(1) Institut Català de Ciències del Clima / Climate Forecasting Unit (IC3/CFU)

(2) Laboratoire de Météorologie Dynamique / Institut Pierre Simon Laplace(LMD/IPSL)

Contact : vguemas@ic3.cat

Mail : Carrer del Doctor Trueta, 203, 08005 Barcelona, Spain

Goal

- What is the impact of a change in latitudinal or longitudinal resolution on the mid-latitude dynamics in the LMDZ atmospheric GCM?
- Which role do the baroclinic waves play in these differing impacts?

Experiments

A
1) **5 ocean/atmosphere coupled experiments** with IPSL-CM (Marti et al., 2010) = LMDZ (atm) + OPA (ocean) + LIM (sea ice) + ORCHDEE (land) : 96x72, 96x96, 144x96, 144x144, 192x144 (= lon x lat)
2) **5 atmosphere forced experiments** (AMIP boundary cond), LMDZ (Hourdin et al., 2006) : 96x72, 96x96, 144x96, 144x144, 192x144

B
3) **11 dynamical-core experiments** following Held & Suarez (1994) design : detailed radiative, turbulence & convective processes replaced by very simple forcing & dissipation : 48x48, 72x48, 96x48, 72x72, 96x72, 144x72, 96x96, 144x96, 96x144, 144x144, 192x144

C
4) **6 dynamical-core constrained sensitivity experiments** in which the zonal-mean zonal-wind is restored toward its daily counterpart from a reference simulation (= the 96x96 free dynamical core experiment) with a timescale of 1day : 72x72, 96x72, 144x72, 96x96, 144x96, 144x144

A - Sensitivity of the full atmospheric model

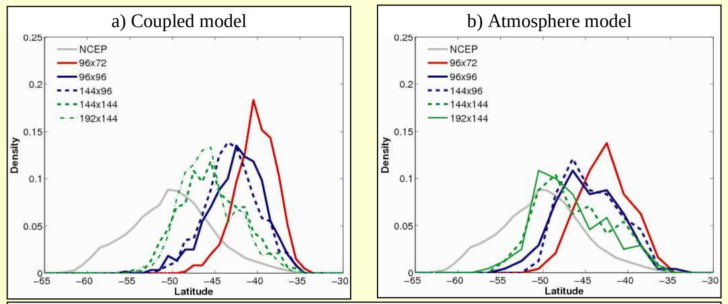

Figure 1 : PDF (Probability Density Function) of the Southern Hemisphere winter jet positions, computed as the latitude of the zonal-mean zonal wind maximum at the 850-hPa level: a) for the five coupled simulations run with the IPSL coupled model b) for the five atmosphere forced simulations run with the LMDZ4 model. The PDF of the winter jet positions in the NCEP data are superimposed in grey.

Increase in latitudinal resolution ⇒ Poleward shift of the jet, increase in variability its position | Not for the longitudinal resolution

B - Dynamical core experiments

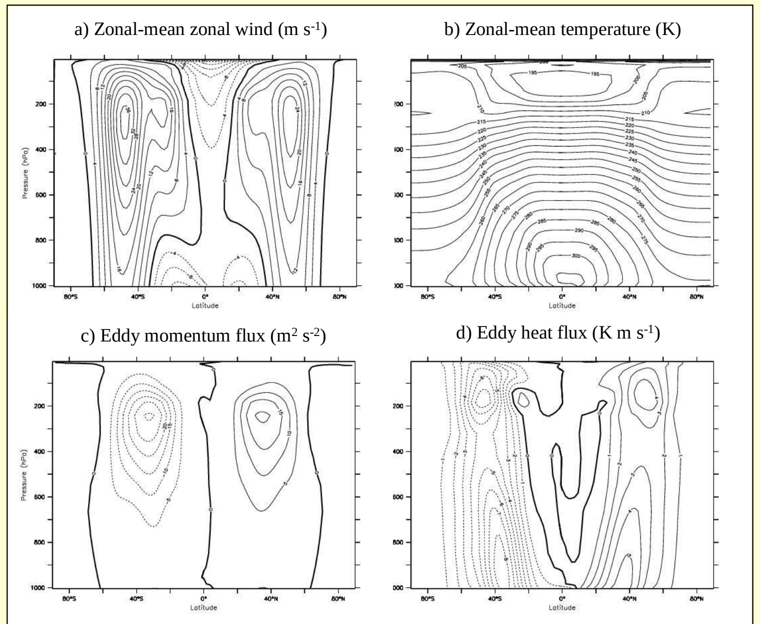

Figure 2 : 96x96 idealized dynamical core experiment: zonal mean of a) Time-mean zonal wind. Contour interval: $4 m.s^{-1}$. b) Time-mean temperature. Contour interval: 5K. c) Eddy momentum flux. Contour interval: $5 m^2.s^{-2}$. d) Eddy heat flux. Contour interval: $1 K.m.s^{-1}$. Continuous (dashed) contours indicate positive (negative) values

Held & Suarez (1994) idealized setup => Realistic mid-latitudinal atmospheric dynamics (Fig. 2)

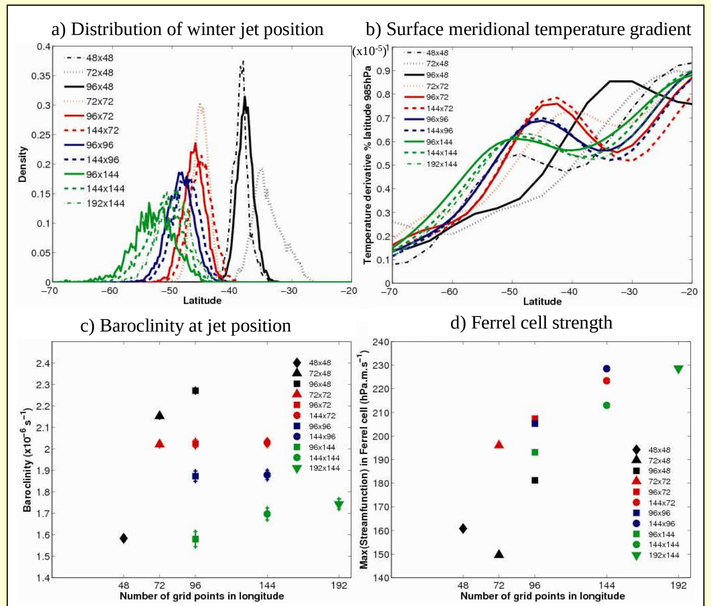

Figure 3 : Free idealized experiments : a) PDF of the winter jet positions, computed as the latitude of the zonal mean zonal wind maximum at the 850hPa level, b) Meridional temperature gradient at the 985hPa level. Units : 10^{-5} K m^{-1}, c) Baroclinity, in s^{-1}, computed between 200hPa and 1000hPa, at the location of the jet, plotted against the number of grid points in longitude, d) Strength of the Ferrel cell, defined as the maximum of the zonal-mean meridional streamfunction, in hPa m s-, as a function of the number of grid points in longitude. In c) and d), the 95% confidence interval is shocn together with the mean value.

Increase in longitudinal resolution :
1) No change in structure & position of the jet (Fig. 3a, b, c)
2) Ferrel cell strengthen (Fig. 3d)
3) More energetic baroclinic waves (Fig.4a, c)

Increase in latitudinal resolution :
1) Poleward shift of the jet + increase in variance of its position as in the full GCM (Fig. 3a)
2) Poleward shift and decrease of the mid-latitude maximum in surface temperature gradient (Fig 3b)
3) Reduced baroclinity (Fig 3c)
4) Poleward shift and less energetic barcolinic wave source (Fig 4a, c)

C – Constrained experiments

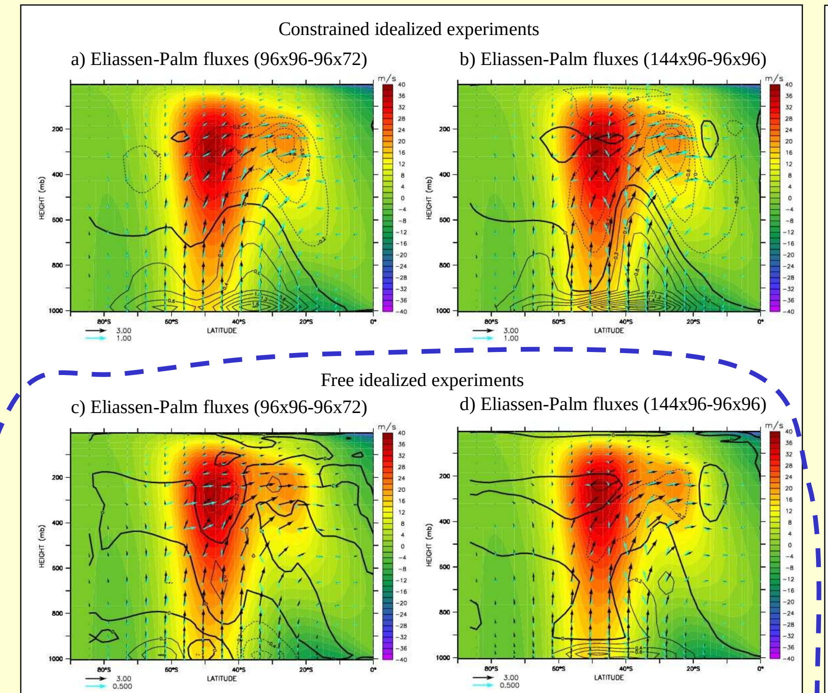

Figure 5: Latitude-pressure cross-sections of Eliassen-Palm fluxes for selected (top) constrained experiments and (bottom) free experiments. Color shading and black arrows: mean zonal wind and Eliassen-Palm fluxes at the 96x96 reference resolution, interval 2 m s^{-1}. Blue arrows and black contours: differences in Eliassen-Palm fluxes and in their divergence between the simulations at (a,c) the 96x96 and 96x72 resolutions, and (b,d) the 144x96 and 96x96 resolutions. Contour interval: 0.2 m s^{-1} day^{-1}, dashed contours negative. The black arrow scale is three times the blue one in a) and b) and six times in c) and d).

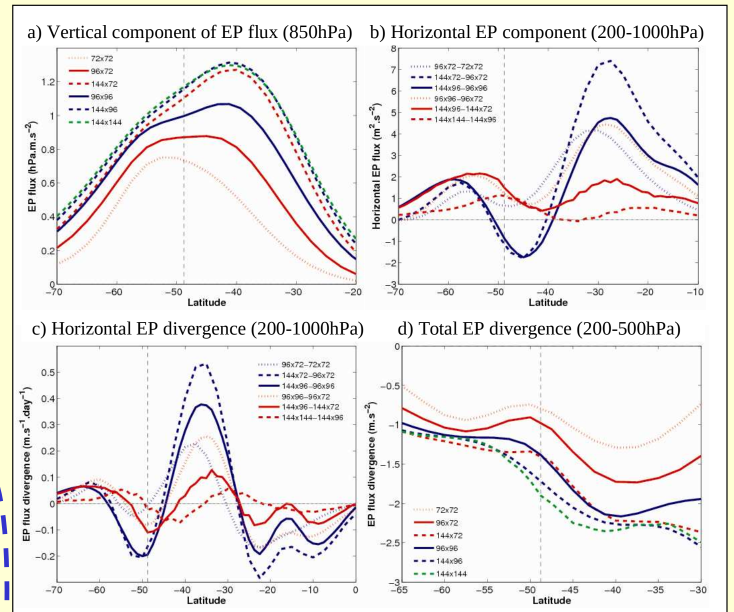

Figure 6 : a, d) Components of the Eliassen-Palm fluxes as a function of latitude for the constrained experiments. b, c) Differences between pairs of simulations, with an increase of the resolution either in latitude (red lines) or in longitude (blue lines); the resolution changes and corresponding linestyles are identical in each panel. (a) Vertical component at the 850hPa level ($hPa.m.s^{-2}$). (b) Horizontal component averaged between 200hPa and 100hPa ($m^2.s^{-2}$). (c) Derivative against the latitude of the horizontal component averaged between 100hPa and 1000hPa ($m.s^{-1}.day^{-1}$). (d) Total divergence of EP flux averaged between 200hPa and 500hPa ($m.s^{-2}$). The vertical black dashed line gives the position of the mid-latitude jet in the constrained experiments.

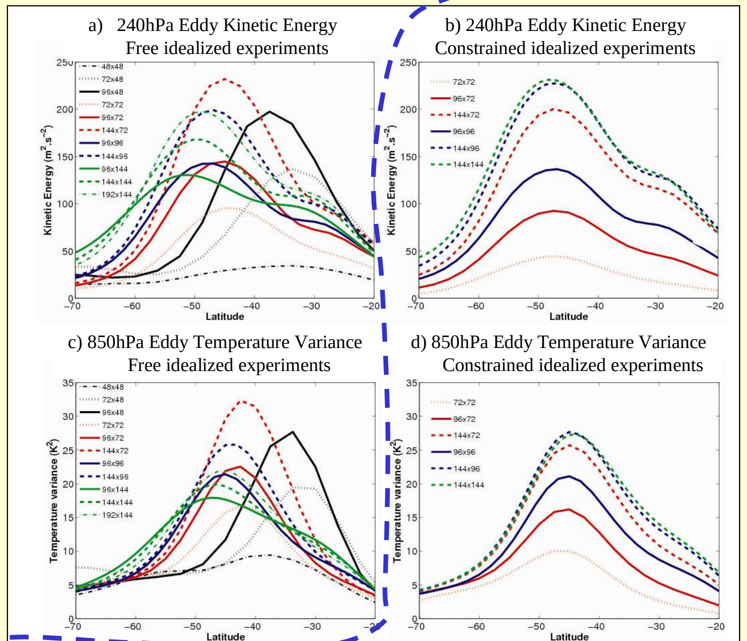

Figure 4 : Time and zonal averages for the free (left) and constrained (right) idealized experiments: a) and b) eddy kinetic energy, at the 240-hPa level, in m^2 s^{-2}, c) and d) eddy temperature variance at the 850-hPa level, in K^2.

Increase in horizontal resolution :
=> More energetic baroclinic waves : increase in EKE, temperature variance & vertical EP flux component (Figs. 4b,d; 6a)

Increase in latitudinal resolution :
=> Amplification of the total fluxes : equatorward propagation, poleward momentum transport (Figs. 5a; 6b, c). Relaxing constraint leads to a poleward jet shift & adjustment of baroclinic wave sources (Fig. 5c)

Increase in longitudinal resolution :
=> Increase in poleward propagation (Fig. 5b,d; 6b, c). Baroclinic waves tend to push the jet equatorward

Increase in horizontal resolution :
=> An equatorward shift of the jet would not be stable (Fig. 6d) according to Robinson (2006) theory (Fig. 7)

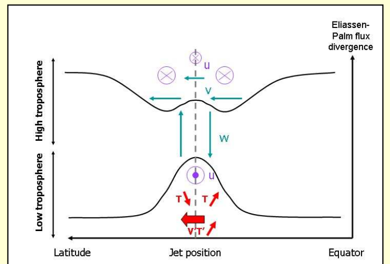

Figure 7: Schematic describing the role of secondary circulations induced by baroclinic waves in the self-maintenance of midlatitudinal jets according to the theory of Robinson et al. (2006)

Conclusions

- An increase in latitudinal resolution induces a poleward shift of the jet, an increase in variance of its position, a reduced baroclinity while an increase in longitudinal resolution leads to a strenghening of the Ferrel cell compensating for more energetic baroclinic waves
- An increase in horizontal resolution leads to more energetic baroclinic waves which propagate equatorward (poleward) if the latitudinal (longitudinal) resolution increases favouring (preventing) a poleward shift of the jet

References :

Held I.M. and M.J. Suarez (1994) A proposal of the dynamical cores of atmospheric general circulation models. *Bull. Amer. Meteor. Soc.*, **75** (10), 1825-1830.

Hourdin F., I Musat, S Bony, P Braconnot, F Codron, J L Dufresne, L Fairhead, M A Filiberti, P Friedlingstein, J Y Grandpeix, G Krinner, P Levan, Z X Li and F Lott (2006) The LMDZ4 general circulation model: climate performance and sensitivity to parametrized physics with emphasis on tropical convection. *Clim. Dyn.*, **27 (7-8)**, 787-813.

Marti O., P Braconnot, J L Dufresne, J Bellier, R Benshila, S Bony, P Brockmann, P Cadule, A Caubel, F Codron, N de Noblet, L Fairhead, T Fichefet, M A Foujols, P Friedlingstein, H Goosse, J Y Grandpeix, E Guilyardi, F Hourdin, A Idelkadi, M Kageyama, G Krinner, C Lévy, G Madec, J Mignot, I Musat, D Swingedouw and C Talandier (2010) Key features of the IPSL ocean atmosphere model and its sensitivity to atmospheric resolution. *Clim. Dyn.*, **34**, 1-26.

Robinson W A (2006) On the Self-Maintenance of Midlatitude Jets. *J. Atmos. Sci.*, **63**, 2109-2122.